ELSEVIER

Journal of Biomechanics 32 (1999) 967–976

JOURNAL OF BIOMECHANICS

www.elsevier.com/locate/jbiomech

# Simulation of initial frontside and backside wear rates in a modular acetabular component with multiple screw holes

Steven M. Kurtz[a,*], Jorge A. Ochoa[b], Chad B. Hovey[a], Christopher V. White[a]

[a]*Exponent Failure Analysis Associates, Inc., 2300 Chestnut Street, Suite 150, Philadelphia, PA 19103, USA*
[b]*Johnson and Johnson Professional, Inc., Raynham, MA, USA*

Received 26 January 1999

**Abstract**

A sliding distance-based finite element formulation was implemented to predict initial wear rates at the front and back surfaces of a commercially available modular polyethylene component during in vitro loading conditions. We found that contact area, contact stress, and wear at the back surface were more sensitive to the liner/shell conformity than the presence of multiple screw holes. Furthermore, backside linear and volumetric wear rates were at least three orders of magnitude less than respective wear estimates at the articulating surface. This discrepancy was primarily attributed to the difference in maximum sliding distances at the articulating surfaces (measured in mm) versus the back surface (measured in μm). This is the first study in which backside wear has been quantified and explicitly compared with frontside wear using clinically relevant metrics established for the articulating surface. The results of this study suggest that with a polished metal shell, the presence of screw holes does not substantially increase abrasive backside wear when compared with the effects of backside nonconformity. 

*Keywords:* Contact stress; Relative motion; Polyethylene: Metal-backing; Acetabular component

## 1. Introduction

Osteolysis in the vicinity of total hip replacements has been associated with the liberation of a critical volume of particulate wear debris, leading to eventual failure of the prosthesis by erosion of the bone–implant interface (Barrack et al., 1997; Dowdy et al., 1997; Kadoya et al., 1998; Perez et al., 1998; Schmalzried et al., 1992,1994; Xenos et al., 1995). In a modular acetabular component, wear debris may be generated at the articulating surface, between the femoral head and the polyethylene liner, or at the back surface, between the liner and the metal shell. Backside wear at the liner/shell interface has been associated with micromotion of the liner and the presence of screw holes (Chen et al., 1995; Cournoyer et al., 1997; Doehring et al., 1996,1997; Lieberman et al., 1996; Williams et al., 1997), and several clinical studies have suggested that backside wear may be a factor leading to focal osteolytic lesions at the bone–implant interface (Bloebaum et al., 1997; Huk et al., 1994).

The back surface of modular acetabular liners may be subjected to abrasion, scratching, gouging, permanent deformation (cold flow), and embedded third body debris during in vivo service (Collier et al., 1992,1990; Guttmann et al., 1994; Huk et al., 1994; Lieberman et al., 1996). In clinical studies, researchers have previously evaluated modular acetabular components by histology of adjacent tissues and by assigning semi-quantitative wear scores to the liners (Bloebaum et al., 1997; Guttmann et al., 1994; Huk et al., 1994). During in vitro studies, metal-backed liners have been assessed by measuring relative motion of the liner relative to the shell, by the plastic deformation of the liner through screw holes, and by estimating the erosion of a thin gold coating on the back surface of the liner (Cournoyer et al., 1997; Doehring et al., 1996,1997; Lieberman et al., 1996; Williams et al., 1997). However, to date backside wear and its relationship to the presence of screw holes has not been quantified in units suitable for comparison with the articulating surface, such as volumetric wear.

Numerical methods have recently been developed to simulate wear at the articulating surface. Using a simple wear model in conjunction with the finite element method, Maxian and colleagues have been able to

* Corresponding author. Tel.: +1-215-751-0973; fax: +1-215-751-0660.

*E-mail address*: skurtz@exponent.com (S.M. Kurtz)

0021-9290/99/$ - see front matter 
PII: S0021-9290(99)00043-3

reproduce clinical trends in average long-term wear rates as a function of head size and successfully predict the outcome of in vitro hip simulator experiments (Maxian et al., 1996a,b,c,1997). The magnitude as well as the distribution of contact stresses at the articulating surface have been shown to be sensitive to slight changes in conformity between the liner and the shell (Kurtz et al., 1993,1994,1998). Thus, changes in backside nonconformity due to the presence of gaps or screw holes might affect wear at both the articulating and back surfaces of a modular component, thereby influencing the risk of osteolysis by changing the total volume of wear debris liberated from the component.

Consequently, the primary goal of this study was to investigate frontside and backside wear in a modular acetabular component using a sliding-distance coupled finite element approach that has previously been shown to simulate wear at the articulating surface. As the foundation of our numerical analyses of backside wear, we employed a finite element model of a modular acetabular component that was previously benchmarked using liner-shell relative motion data collected during in vitro mechanical testing (Kurtz et al., 1998). In the present study, we explored the hypothesis that backside nonconformity plays as important role in the total wear of a modular acetabular component as the presence of multiple screw holes.

## 2. Materials and methods

Three-dimensional finite element models were constructed from design drawings of a commercially available modular acetabular component system with an inner diameter of 28 mm, a thickness of 7.8 mm, and an overall outer diameter of 54 mm (PFC Acetabular Component, Johnson and Johnson Professional, Inc., Rayhnam, MA). The models all consisted of three contacting parts, including the femoral head, the acetabular liner, and the metal shell (Fig. 1). A total of six models were generated for the present study, including two distinct backside conformities and three different fenestrated shell designs.

The polyethylene liner was modeled as either perfectly conforming on nonconforming with the metal shell. When the liner was nonconforming with the shell, as-manufactured tolerances were assigned to the spherical, equatorial, and rim regions of the model (Kurtz et al., 1998). In all of the models, the femoral head was modeled with a 0.1 mm radial clearance with the articulating surface of the liner.

Three different shell models were considered with varying fenestrations: (1) no hole, (2) two hole, and (3) eight hole designs. All three design variations had a 4.0 mm radius polar fenestration and (in the two hole and eight hole models) screw holes of 4.95 mm radius. The locations of the screw holes are summarized in Table 1. The geometry of the no hole design was detailed previously (Kurtz et al., 1998), whereas the finite element meshes for the two hole and eight hole shell designs are depicted in Fig. 2A and B, respectively.

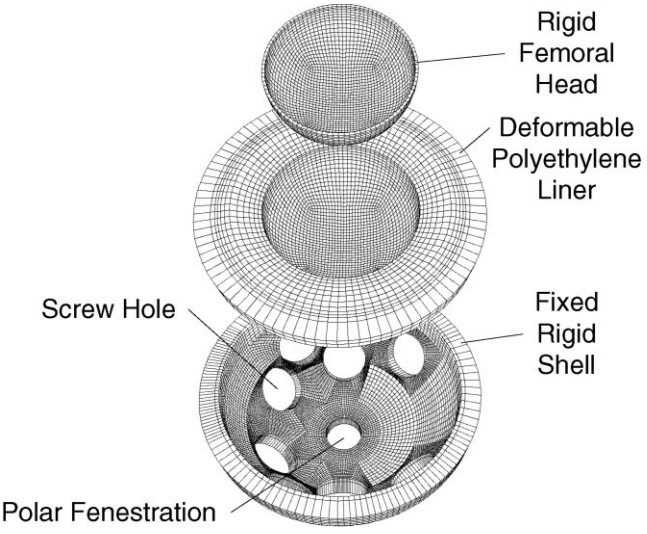


Fig. 1. Exploded view of the finite element model, illustrating parts representing the rigid femoral head, the deformable polyethylene liner, and the rigid metal shell.

Table 1
Screw hole locations and sizes for no hole, two hole, and eight hole configurations

| Shell design parameter | No hole | Two hole | Eight hole |
|---|---|---|---|
| Polar fenestration radius (mm) | 4.00 | 4.00 | 4.00 |
| Screw hole radius (mm) | N/A | 4.95 | 4.95 |
| Screw hole 1 inclination angle (°) | N/A | 45 | 45 |
| Screw hole 1 azimuthal angle (°) | N/A | ± 30 | ± 30 |
| Screw hole 2 inclination angle (°) | N/A | N/A | 60 |
| Screw hole 2 azimuthal angle (°) | N/A | N/A | ± 60 |
| Screw hole 3 inclination angle (°) | N/A | N/A | 45 |
| Screw hole 3 azimuthal angle (°) | N/A | N/A | ± 90 |
| Screw hole 4 inclination angle (°) | N/A | N/A | 60 |
| Screw hole 4 azimuthal angle (°) | N/A | N/A | ± 135 |

The femoral head and the shell were modeled as rigid bodies. The polyethylene liner was modeled as a linear elastic, isotropic material with an elastic modulus of 974 MPa and Poisson's ratio of 0.46. Frictional contact at the head–liner and liner–shell interfaces was assumed to be Coulombic with a frictional coefficient of 0.083. Material model parameters were based on the scientific literature, as documented in our previous benchmarking study (Kurtz et al., 1998). The same friction coefficients were used at the front and back surfaces of the component to model polished conditions at the head/liner and liner/shell interfaces.

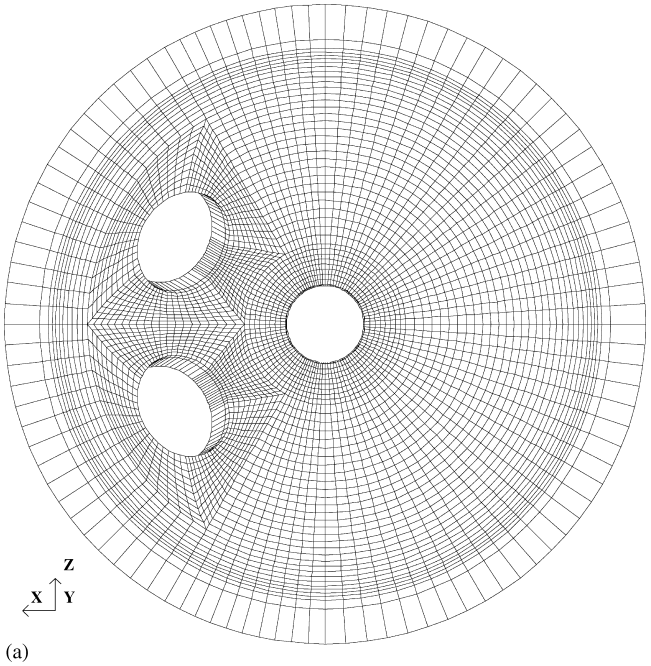


(a)

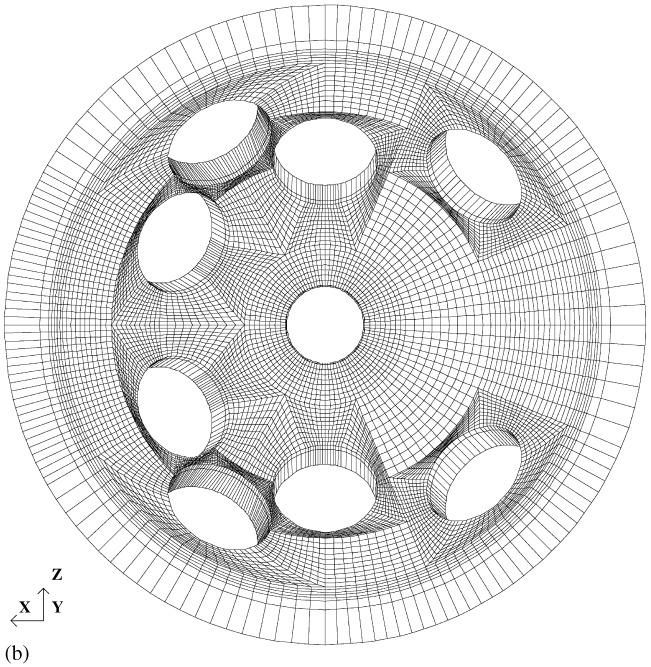


(b)

Fig. 2. Top views of the finite element mesh for the (a) two-hole model and (b) eight hole model of the acetabular shell.

Equatorial and rim restraints on the liner were employed to simulate idealized locking mechanisms, as shown in Fig. 2 of the earlier benchmarking study (Kurtz et al., 1998). In all simulations, selected finite element nodes at the rim had zero displacements perpendicular to the polar axis to simulate the cardinal locking tabs at the rim. Similarly, selected nodes at the equator had zero displacements parallel to the polar axis to simulate the locking ring at the equator.

At the center of gravity of the femoral head a point load representing the Paul load curve was imposed with a peak of 3012 N, based on data collected during in vitro mechanical testing (Cournoyer et al., 1997). The femoral head load was applied at an inclination of 40° and anteversion of 15° with respect to the liner, as specified by the manufacturers implantation instructions; the loading direction was illustrated in Fig. 2 of our earlier study (Kurtz et al., 1998). For our present simulations, the Paul curve was discretized into 14 time intervals (Fig. 3), and the magnitude, but not the orientation, of the load was varied as a function of time, consistent with the previous in vitro testing (Cournoyer et al., 1997). Dynamic relaxation, as detailed by Underwood (1983), was used to solve the quasi-static three-body contact problem using a commercially available structural dynamics code (LS-DYNA3D, Livermore Software Technology Corporation, Livermore, CA), as described previously (Kurtz et al., 1998).

The finite element mesh of the shell, liner, and head consisted of eight-noded hexagonal solid elements (Table 2). A mesh refinement study verified convergence of the quasi-static contact solution, and our prior benchmarking study confirmed the accuracy of the predicted backside relative motion between the liner and shell (Kurtz et al., 1998). Mesh refinement near the vicinity of the screw holes captured the localized stress concentrations arising from these holes. Simulations were performed on a Silicon Graphics Origin 200 workstation with a single 180 MHz R10000 CPU. Table 2 shows the solution times for each model.

Script files were used to automate mesh generation in ANSYS v5.3 (ANSYS Inc., Houston, PA). In the absence of a fully featured translator from ANSYS v5.3 to LS-DYNA3D, the node, element, and constraint information from ANSYS was augmented by custom keyword files to create complete LS-DYNA3D-ready files. A single structural analysis run yielded both frontside and backside pressure data, thus a total of 12 subsequent wear analyses were performed.

The calculation of backside wear, calculated with custom software developed in the C programming language, was based on the nodal displacements and nodal normal contact pressures for the backside interface between the metal shell and the polyethylene liner (See Table 3). Backside wear depth (WD) was computed for each backside node using a discretized form of the Archard wear equation proposed by Maxian et al., 1996b. Fig. 5 shows a flowchart describing how wear calculations were made. The wear depth at any time $t$,

$$WD_t(\theta, \phi) = k\sigma_t(\theta, \phi) \times s_t(\theta, \phi) \quad (1)$$

depends on a wear constant $k$, local normal stress $\sigma_t(\theta, \phi)$, and the local sliding distance $s_t(\theta, \phi)$. The wear coefficient, independent of position $(\theta, \phi)$ and time $t$, was

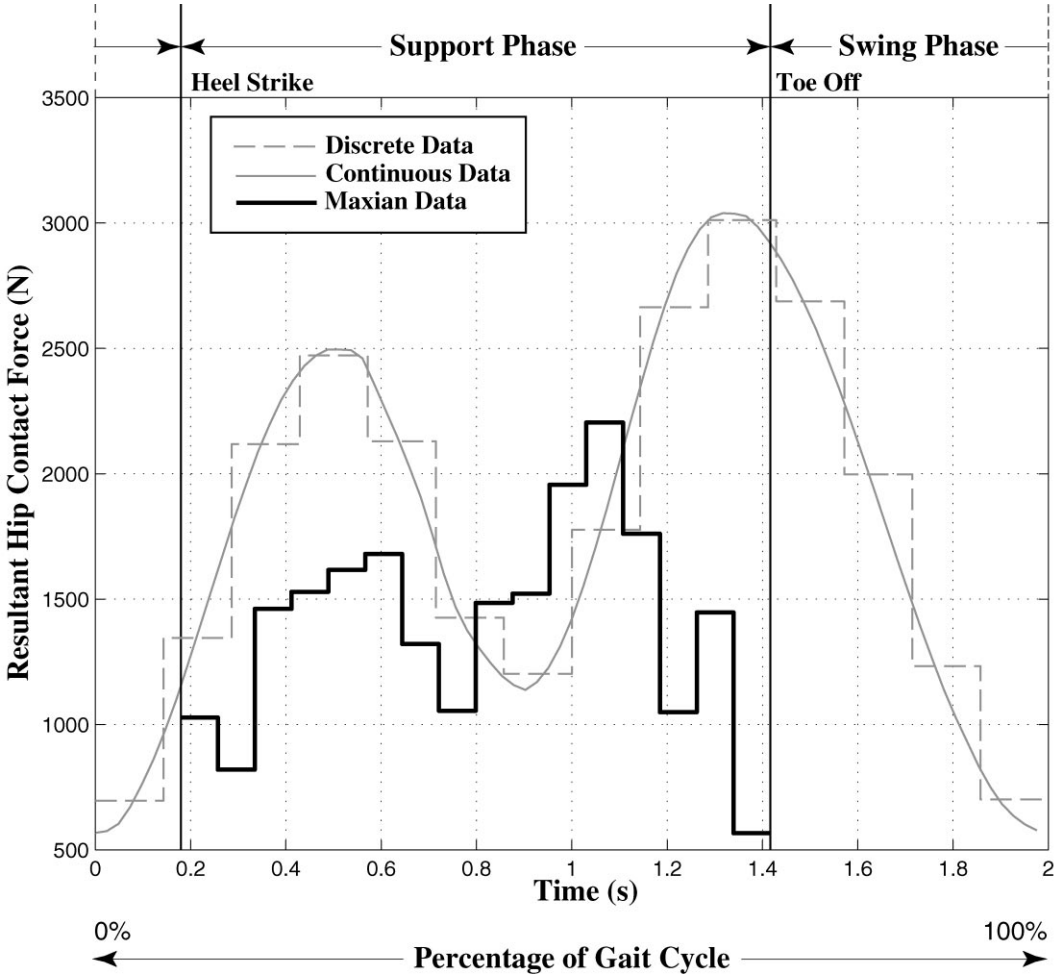


Fig. 3. Load time history, taken from in vitro mechanical testing (Cournoyer et al., 1997) compared to the load time history from Maxian et al. (1996c) in bold. Note that Maxian uses only the support phase of gait, whereas this study used the entire gait cycle-the support phase and the stance phase.

Table 2
Number of nodes, elements, and solution time for each model

| Shell variation | Number of elements | Number of nodes | Solution time (h) |
|---|---|---|---|
| No hole | 34,560 | 44,893 | 35.3 |
| Two hole | 34,728 | 45,175 | 36.1 |
| Eight hole | 43,664 | 59,473 | 43.5 |

assumed to be $10.656 \times 10^{-7}\,\mathrm{mm^3\,N^{-1}\,m^{-1}}$ for comparison with Maxian et al. (1996a,b,c). The normal stress and sliding distance depended on the position of a node on the contacting surface. During a given time step, the wear volume (WV) was calculated as the average wear depth of the four surface nodes multiplied by the area of the $e$th element face in contact ($A^e$)

$$WV_t^e(\theta, \phi) = \sum_{j=1}^{4} WD(\theta, \phi, t) \times A^e/4. \quad (2)$$

Total wear depth for a particular node was calculated as the sum of incremental wear depth at each time step,

$$WD(\theta, \phi) = \sum_{t=1}^{n_{ts}} WD_t(\theta, \phi), \quad (3)$$

where $n_{ts}$, the number of time steps, was 14 (Figs. 3 and 4). Total wear volume for a backside element was calculated in an analogous manner

$$WV^e(\theta, \phi) = \sum_{t=1}^{n_{ts}} WV_t^e(\theta, \phi). \quad (4)$$

Finally, total volumetric wear for the entire backside ($W$) was calculated by adding the contributions from all $n_{el}$ backside elements:

$$W = \sum_{e=1}^{n_{el}} WV^e(\theta, \phi). \quad (5)$$

In contrast to backside wear calculations, which used liner-relative-to-shell displacements calculated from the finite element analysis, frontside wear calculations used

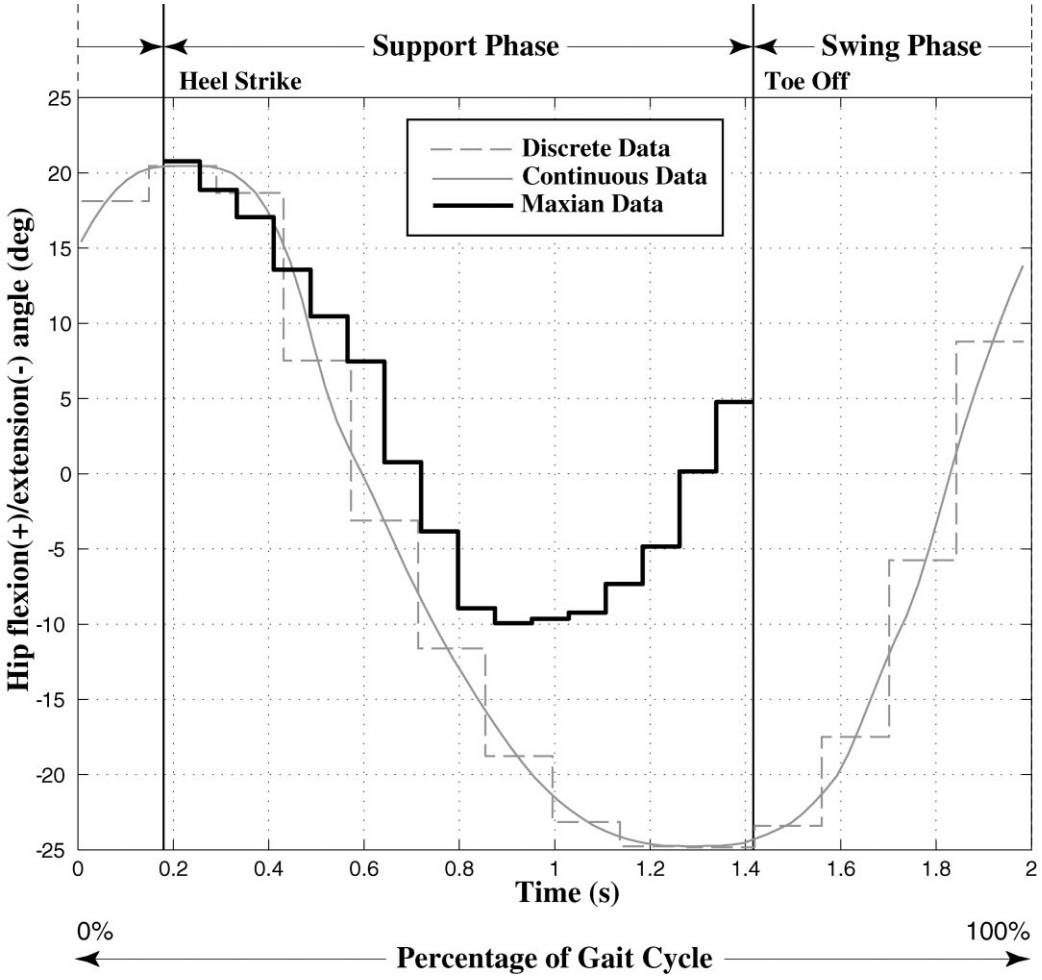


Fig. 4. Hip flexion/extension time history, taken from in vitro mechanical testing (Cournoyer et al., 1997) compared to the load time history from Maxian et al. (1996c) in bold.

Table 3
Summary of backside (Liner/Shell) interface results

| Design | Shell | Contact area | Contact stress | Linear wear | Volumetric wear |
|---|---|---|---|---|---|
| No hole | NC | 574 | 10.01 | $3.36\times10^{-4}$ | $4.18\times10^{-2}$ |
| No hole | C | 2395 | 7.86 | $1.37\times10^{-4}$ | $6.65\times10^{-2}$ |
| Two hole | NC | 531 | 11.09 | $3.65\times10^{-4}$ | $4.22\times10^{-2}$ |
| Two hole | C | 2247 | 9.14 | $1.18\times10^{-4}$ | $5.55\times10^{-2}$ |
| Eight hole | NC | 487 | 11.09 | $3.58\times10^{-4}$ | $3.92\times10^{-2}$ |
| Eight hole | C | 1711 | 9.54 | $1.35\times10^{-4}$ | $5.23\times10^{-2}$ |

Maximum contact area ($mm^3$), Maximum contact stress (MPa), Initial linear wear rate (mm/year), and Volumetric wear rate ($mm^3$/year). C = Conforming shell; NC = Nonconforming shell.

liner-relative-to-femoral head displacements calculated from rigid body kinematics, consistent with (Maxian et al., 1996a,b,c,1997) (see Fig. 5). Using Maxian's computational scheme, frontside wear depth was computed at each nodal location as the product of contact stress (from quasi-static finite element analysis) with incremental sliding distance (from rigid body femoral head kinematics).

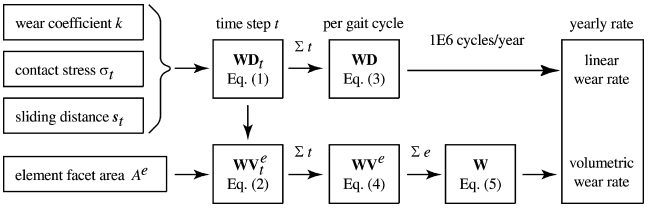


Fig. 5. Flowchart describing how wear calculations were constructed.

In this study, femoral head kinematics were prescribed, using simple rotation in the sagittal plane from $+20^\circ$ (flexion) to $-25^\circ$ (extension) based on experimental data from previous in vitro mechanical testing (Cournoyer et al., 1997). The continuous flexion/extension data were discretized into 14 increments, consistent with the loading duty cycle used for the finite element simulations (Fig. 4). Incremental nodal sliding distances were calculated using Matlab v.5 (The Math Works, Inc., Natick, MA)

based on the fixed orientation of the acetabular component relative to the pelvis and the incrementally varying orientation of the femoral head relative to the pelvis. A custom C-program was developed to compute frontside wear based on the contact pressures obtained from the finite element analysis and the relative sliding distances computed based on rigid body femoral head kinematics. Consistent with Maxian's research, a wear coefficient of $10.656 \times 10^{-7}$ $mm^3N^{-1}$ $m^{-1}$ was used in the frontside wear calculations. A validation study, detailed in the Appendix, was performed to verify the custom code used to calculate frontside wear.

## 3. Results

Contact area, contact stress, and wear at the liner/shell interface were more sensitive to liner/shell conformity than the presence of screw holes (Figs. 6 and 7, Table 1). For example, increasing the conformity of the back surface decreased the linear wear by 59% in the no hole design; in contrast, adding two screw holes to the no hole design increased the linear wear by only 9% (Table 1). Although increasing the number of screw holes reduced the inner surface area of the shell, the backside area in contact with the liner under peak loading was not appreciably affected when nonconformity was present at the liner/shell interface (Table 1). Wear rates for the two hole and eight hole designs were not substantially different, because the additional screw holes fell outside the region of primary liner–shell load transfer.

Backside linear and volumetric wear rates were three and four orders of magnitude less, respectively, than wear estimates at the articulating surface (Table 2). This discrepancy was primarily attributed to the difference in maximum sliding distances at the articulating surface (measured in mm) versus the back surface (measured in μm). Frontside contact area, contact stress, and linear wear rates, as well as the distribution of initial wear at the articulating surface were all sensitive to liner/shell conformity than the presence of screw holes (Figs. 8 and 9, Table 2). However, volumetric wear at the articulating surface was insensitive to both backside nonconformity and the presence of screw holes.

## 4. Discussion

Our results show frontside wear to be substantially larger than backside wear, underscoring the primary importance of frontside wear considerations for design purposes. Our results also suggest that when the metal

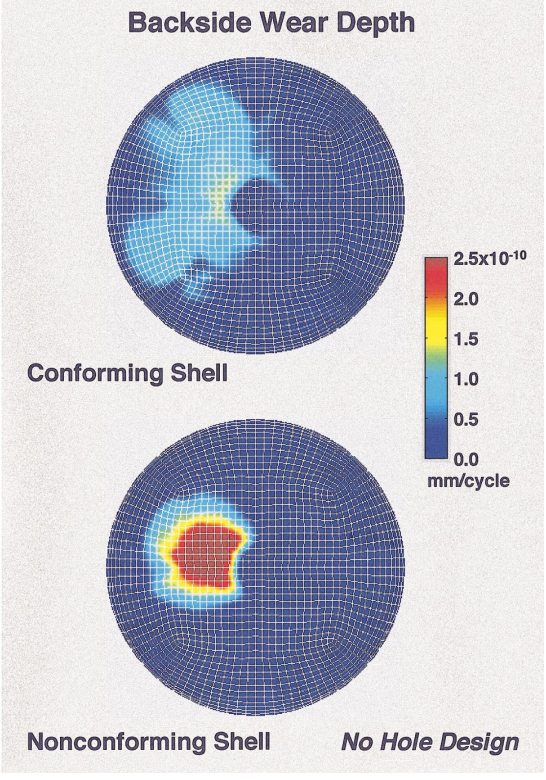


Fig. 6. Backside wear for the no hole shell design with (A) nonconforming and (B) conforming liners. Note the concentration of wear in the vicinity of the polar fenestration in the conforming case.

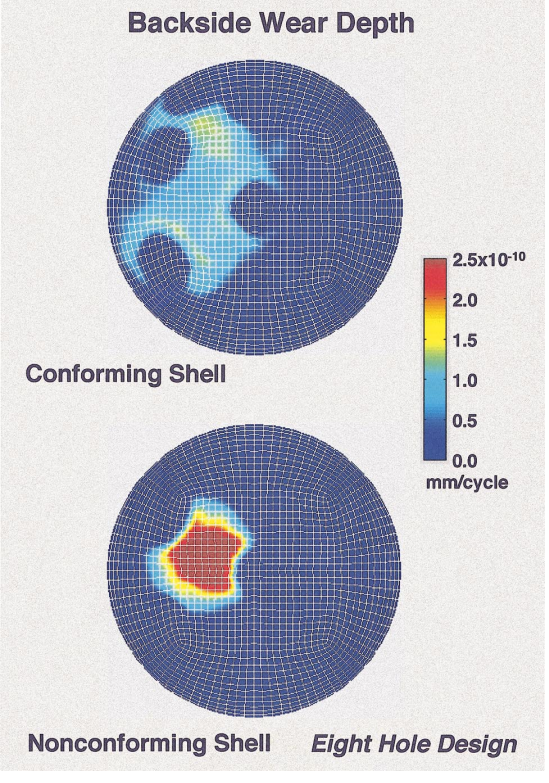


Fig. 7. Backside wear for the eight hole shell design with (A) nonconforming and (B) conforming liners. Note the concentration of wear in the vicinity of the polar fenestration and screw holes for the conforming case.

shell is polished, the presence of screw holes does not substantially increase abrasive backside wear when compared with the effects of backside nonconformity. This study further demonstrates that an abrasive wear model, in conjunction with the finite element method, can be an effective tool by which to quantitatively evaluate design variables and their hypothesized effects on initial backside wear rates.

This study is limited to initial wear rates. Long-term backside wear of the polyethylene in the presence of screws, screw holes, and other nonconforming geometries may influence the clinical performance of a modular acetabular component at the bone–implant interface (Bloebaum et al., 1997; Huk et al., 1994). This work is still clinically relevant, however, because it is the first study in which backside wear has been quantified and explicitly compared with frontside wear using metrics established for the articulating surface. The validation of backside wear with clinical and numerical frontside wear data is critical for future backside wear investigations accounting for long-term wear.

Adaptive remeshing used for long-term, frontside wear simulation to account for substantial geometric head–liner changes may not be as essential to backside wear simulation. Changes in backside nonconformity are more likely to occur due to creep rather than wear, as suggested in Williams et al. (1997), which demonstrated progressive changes to liner–shell relative motion during an in vitro examination of five designs loaded for up to $10^7$ cycles. Although the sensitivity of our results to changes in conformity illustrates the importance of accounting for long-term geometric changes in the backside geometry, these changes can be simulated using time-dependent constitutive behavior for polyethylene, not remeshing.

Due to limitations of the wear theory, the conclusions of this study are applicable to a polished backside interface with homogenous tribological properties. Such conditions may not apply in the vicinity of screw holes with sharp edges, where focal wear has been clinically observed (Huk et al., 1994). Although the inner surface of the metal shell may be manufactured with a matte finish, the wear coefficient for polyethylene against this type of counterface has yet to be determined. Thus, our present study was limited to evaluation of polished interface conditions, for which both friction and wear coefficients have previously been established.

Though our results show nonconformity to be as important as the presence of screw holes to backside wear, the presence of screws (not included as a parameter in this study) may be critical depending on whether or not the screws are fully seated and flush with the bottom of the screw hole, or canted (i.e., not parallel) with respect to

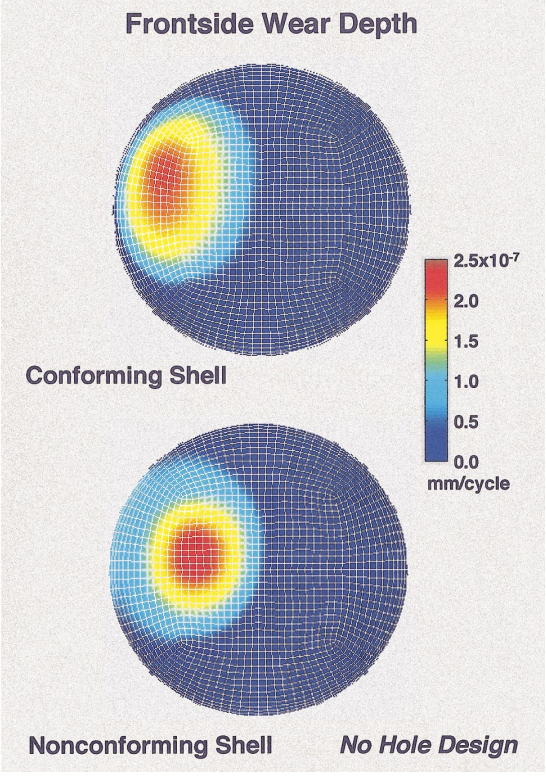


Fig. 8. Frontside wear for the no hole shell design with (A) nonconforming and (B) conforming liners. Despite the sensitivity of the wear distributions to backside conformity, the overall volumetric wear rate did not change substantially.

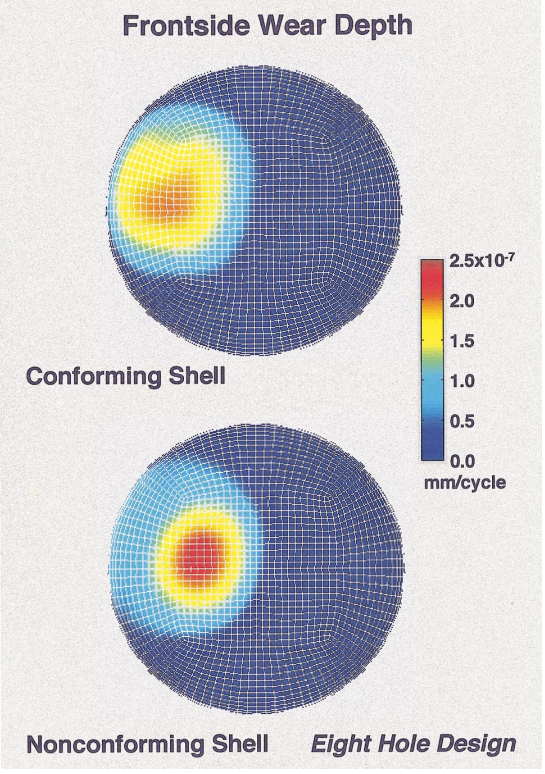


Fig. 9. Frontside wear for the eight hole shell design with (A) nonconforming and (B) conforming liners. Despite the sensitivity of the wear distributions to backside conformity, the overall volumetric wear rate did not change substantially.

the screw hole and impinging on the back surface of the polyethylene liner. Postmortem observations by Bloebaum et al. (1997) found no significant difference between the presence of empty screw holes and seated screws with the prevalence of osteolysis. In contrast, they reported significantly higher prevalence of osteolysis associated with canted screws than with empty holes. Thus, the results of the present study may be applicable to occupied screw holes, provided the screws are seated, not canted.

Another important limitation of this study was the simplified Archard wear model. Wear at the articulating surface is known to depend not only on the multidirectional motion at the articulating surface (Jasty et al., 1997; Wang et al., 1997), but also upon the applied load in a nonlinear manner (Wang et al., 1995). Thus, the Archard model likely oversimplifies the complex tribological conditions at the articulating surface. Nevertheless, as Maxian's work has shown, the Archard theory can provide reasonable estimates of average clinical wear rates and in vitro hip simulator results when used with a properly validated finite element model.

An unexpected result of this study was the finding that frontside volumetric wear rates were insensitive to both backside nonconformity and the number of screw holes. Variations in the backside geometry were observed to affect the maximum contact stress, contact area, and linear wear rate at the articulating surface. Overall, however, these individual effects were not apparent from the calculated value of the volumetric wear because of variations in tangential displacements. Although the loading conditions and femoral head kinematics were simplified for the present study for the purposes of consistency with previous in vitro mechanical testing, based on the results of our validation study, these assumptions are not expected to influence our overall finding that frontside wear predominates over backside wear in a nearly conforming liner design with polished conditions at both interfaces.

In general, the frontside linear and volumetric wear results from this study were approximately two times higher than the published results by Maxian et al. (Tables 4 and 5). However, several factors make this study intrinsically different from Maxian's:

1. Hip excursion data for flexion/extension from the *in vitro* mechanical testing ranged from $+20^\circ$ to $-25^\circ$ whereas Maxian's data ranged from $+20^\circ$ to $-10^\circ$. The larger excursions in the present study translated into higher wear predictions.
2. The present study included the full gait cycle (support phase and swing phase) whereas Maxian only included the support phase. Again, this translated into higher wear rates for the current study.
3. Our load magnitudes (and thus resulting pressures) were higher in the present study than in Maxian's, which logically led to higher wear rates. In this study, load magnitudes varied between 500 and 3000 N whereas Maxian used loads between 500 and 2000 N.

Table 4
Summary of Frontside (Head/Liner) Interface Results

| Design | Shell | Contact area | Contact stress | Linear wear | Volumetric wear |
|---|---|---|---|---|---|
| No hole | NC | 559 | 16.88 | 0.229 | 39.0 |
| No hole | C | 499 | 13.44 | 0.212 | 38.6 |
| Two hole | NC | 573 | 16.95 | 0.227 | 39.0 |
| Two hole | C | 524 | 12.21 | 0.193 | 38.6 |
| Eight hole | NC | 561 | 16.97 | 0.226 | 37.4 |
| Eight hole | C | 518 | 12.74 | 0.200 | 38.5 |

Maximum contact area ($mm^3$), Maximum contact stress (MPa), Initial linear wear rate (mm/year), and Volumetric wear rate ($mm^3$/year). C = Conforming shell, NC = Nonconforming shell.

Table 5
Comparison of the initial frontside wear results from the validation study in the appendix to those published by Maxian et al. (1996c)

| Wear quantity (initial rates) | Validation study | Maxian study |
|---|---|---|
| Maximum linear wear rate (mm/yr) | 0.119 | 0.111 |
| Maximum volumetric wear rate ($mm^3$/yr) | 15.9 | 16 |

Furthermore, when Maxian's inputs were employed in the wear calculations instead of those obtained from in vitro testing, reasonable agreement was obtained with Maxian's published results, as summarized in Table 5 and detailed by the Appendix.

The computational wear results compare favorably with the broad range of clinically reported wear rates for total hip arthroplasty. As summarized by Sauer and Anthony (1998) in a recent review article, the average volumetric wear for a 28 mm diameter CoCr head articulating against a polyethylene liner has been reported to range from 48 to 139 $mm^3$ per year across four studies, corresponding to a mean of 85 $mm^3$ per year and standard deviation of 33 $mm^3$ per year. Sauer and Anthony (1998) identified 34 independent wear-related parameters, including contact-, lubricant-, counterface-, patient-, UHMWPE- and measurement-related factors to explain the variability of wear rates reported in the clinical literature. In comparison, the computed front-side wear rates were, on average, 39 $mm^3$ per year in the present study and 16 $mm^3$ per year in Maxian et al. (1996c). Thus, the computationally obtained frontside volumetric wear rates in the present study fall within the broad envelope of previous clinical observations.

Validated wear simulations provide an opportunity to address liner–shell design questions that are currently beyond the scope of existing clinical data and in vitro

wear simulators. In the present study, we were able to determine that backside nonconformity plays as important a role as the presence of screw holes in the initiation of initial backside polyethylene wear. Ultimately, numerical wear simulations are expected to improve design evaluations during the development of future modular acetabular components for total hip arthroplasty.

## Acknowledgements

Supported by a Research Grant from Johnson and Johnson Professional, Inc. Thanks to S. Srivastav for his technical assistance.

## Appendix A. Frontside wear validation

The purpose of this appendix was to validate the custom software that was developed to calculate initial wear rates. For the validation study, femoral head loading and hip kinematics were obtained from the research by Maxian and colleagues and used as input to our custom code. Using an approach similar to that of Estupiñán and coworkers (Estupiñán et al., 1997), we obtained our contact stress distributions for the validation study using the elastic contact solution of a rigid femoral head indenting an elastic acetabular liner (Bartel et al., 1985). We adopted this simplified approach for the validation study because in Maxian's models, the liner was perfectly conforming with the metal shell (there were no screw holes), and Estupiñán showed that initial frontside wear calculations based on the theoretical contact solutions were in agreement with finite element predictions, assuming liner conformity with the metal shell and no screw holes (Estupiñán et al., 1997). We verified our implementation of the theoretical contact stress calculations using previously published solutions (Bartel et al., 1985).

In Maxian's article (Maxian et al., 1996c), the load direction was assumed to vary for each time step in the anterior/posterior, medial/lateral, and superior/inferior directions. In the present validation study, the magnitude of Maxian's load vector varied from step to step, but the direction was assumed to be aligned with the polar axis for all time steps. This simplification was not expected to critically alter our results because for both our study and that of Maxian's, the tangential displacement field (i.e., sliding distances) did not vary substantially within the area of contact, as determined by analysis of the femoral head kinematics. Furthermore, previous finite element analyses have suggested that the contact stress distributions in acetabular components are not substantially affected by changes in load orientation of less than 45° from the polar axis (Schmidt and Bartel, 1997).

The mesh for the No Hole conforming frontside geometry was used for the validation study, because of its similarity to that considered previously (Maxian et al., 1996c). The load magnitude and hip excursion time histories used by Maxian are illustrated in Figs. 3 and 4. For consistency with Maxian's study, we used an elastic modulus of 1400 MPa and a Poisson's ratio of 0.3 in the theoretical contact stress calculations at each time step. Consistent frontside incremental sliding displacements were calculated for 45° inclination and 0° anteversion. Using these contact stress and sliding distance calculations, we used our custom software to determine the initial wear rate based on 1,000,000 gait cycles per year. The wear calculations from the validation study coincided very well with those previously published (Maxian et al., 1996c), verifying our methodologies to be correctly implemented (Table 5).

During the validation study, the theoretical elastic contact solution provided a convenient method of estimating initial frontside wear rates without performing the time-intensive finite element analyses. Estupiñán and coworkers employed a similar methodology to calculate the initial wear coefficient at the articulating surface (Estupiñán et al., 1997). Using the kinematics of a biaxial rocking hip simulator and the elastic contact solution, Estupiñán et al. determined the wear coefficient to be $29.3 \times 10^{-7}\,\mathrm{mm^3\,N^{-1}\,m^{-1}}$, nearly three times larger than that employed by Maxian and colleagues (1996c), who based their original wear coefficient on extrapolated data from pin-on-disk studies. More recently, Maxian and coworkers performed a validation of their frontside wear analyses against a biaxial rocking hip simulator, obtaining a wear coefficient of $15.5 \times 10^{-7}\,\mathrm{mm^3\,N^{-1}\,m^{-1}}$ (Maxian et al., 1997). These studies underscore the importance of model validation, as institutional variation in wear testing conditions apparently plays an important role in wear coefficient determination.

## References

Barrack, R.L., Folgueras, A., Munn, B., Tvetden, D., Sharkey, P., 1997. Pelvic lysis and polyethylene wear at 5–8 years in an uncemented total hip. Clinical Orthopaedics 335, 211–217.

Bartel, D.L., Burstein, A.H., Toda, M.D., Edwards, D.L., 1985. The effect of conformity and plastic thickness on contact stresses in metal-backed plastic implants. Journal of Biomechanical Engineering 107, 193–199.

Bloebaum, R.D., Mihalopoulus, N.L., Jensen, J.W., Dorr, L.D., 1997. Postmortem analysis of bone growth into porous-coated acetabular components. Journal of Bone and Joint Surgery, American 79, 1013–1022.

Chen, P.C., Mead, E.H., Pinto, J.G., Colwell, C.W., Jr., 1995. Polyethylene wear debris in modular acetabular prostheses. Clinical Orthopaedics, 44–56.

Collier, J.P., Mayor, M.B., Jensen, R.E., Surprenant, V.A., Surprenant, H.P., McNamar, J.L., Belec, L., 1992. Mechanisms of failure of modular prostheses. Clinical Orthopaedics 285, 129–139.

Collier, J.P., Mayor, M.B., Surprenant, V.A., Surprenant, H.P., Dauphinais, L.A., Jensen, R.E., 1990. The biomechanical problems of polyethylene as a bearing surface. Clinical Orthopaedics 261, 107–113.

Cournoyer, J.R., Ochoa, J.A., Kurtz, S.M., 1997. Relative motion at the backside of a metal-backed acetabular component under quasistatic and dynamic loading. Transactions of Orthopaedics Research Society 22, 839.

Doehring, T.C., Saigal, S., Shanbhag, A.S., Rubash, H.E., 1996. Micromotion of acetabular liners: Measurements comparing the effectiveness of locking mechanisms. Transactions of Orthopaedics Research Society 21, 427.

Doehring, T.C., Wentz, M.J., Shanbhag, A.S., Rubash, H.E., 1997. The effect of UHMWPE liner geometry on micromotion. Transactions of Orthopaedics Research Society 22, 52.

Dowdy, P.A., Rorabeck, C.H., Bourne, R.B., 1997. Uncemented total hip arthroplasty in patients 50 years of age or younger. Journal of Arthroplasty 12, 853–862.

Estupiñán, J.A., Furman, B.D., Li, S., Bartel, D.L., 1997. Wear coefficient for reference UHMWPE in a biaxial rocking hip simulator. 1997 Bioengineering Conference (ASME) 35, 159–160.

Guttmann, D., Schmalzried, T.P., Kabo, J.M., Amstutz, H.C., 1994. 40th Orthopedic Research Society, p. 178.

Huk, O.L., Bansal, M., Betts, F., Rimnac, C.M., Lieberman, J.R., Huo, M.H., Salvati, E.A., 1994. Polyethylene and metal debris generated by non-articulating surfaces of modular acetabular components. Journal of Bone and Joint Surgery, American 76, 568–574.

Jasty, M., Goetz, D.D., Bragdon, C.R., Lee, K.R., Hanson, A.E., Elder, J.R., Harris, W.H., 1997. Wear of polyethylene acetabular components in total hip arthroplasty. An analysis of one hundred and twenty-eight components retrieved at autopsy or revision operations. Journal of Bone and Joint Surgery, American 79, 349–358.

Kadoya, Y., Kobayashi, A., Ohashi, H., 1998. Wear and osteolysis in total joint replacements. Acta Orthopaedical Scandinavica Supplimentary 278, 1–16.

Kurtz, S.M., Bartel, D.L., Edidin, A.A., 1994. The effect of gaps on contact stress and relative motion in a metal-backed acetabular component. Transactions of Orthopaedics Research Society 19, 243.

Kurtz, S.M., Gabriel, S.M., Bartel, D.L., 1993. The effect of nonconformity between metal backing and polyethylene inserts in acetabular components for total hip arthroplasty. Transactions of Orthopaedics Research Society 18, 434.

Kurtz, S.M., Ochoa, J.A., White, C.V., Srivastav, S., Cournoyer, J., 1998. Backside nonconformity and locking restraints affect liner/shell load transfer mechanisms and relative motion in modular acetabular components for total hip replacement. Journal of Biomechanics 31, 431–437.

Lieberman, J.R., Kay, R.M., Hamlet, W.P., Park, S.H., Kabo, J.M., 1996. Wear of the polyethylene liner-metallic shell interface in modular acetabular components. An in vitro analysis. Journal of Arthroplasty 11, 602–608.

Maxian, T.A., Brown, T.D., Pedersen, D.R., Callaghan, J.J., 1996a. Adaptive finite element modeling of long-term polyethylene wear in total hip arthroplasty. Journal of Orthopaedic Research 14, 668–675.

Maxian, T.A., Brown, T.D., Pedersen, D.R., Callaghan, J.J., 1996b. The Frank Stinchfield Award. 3-Dimensional sliding/contact computational simulation of total hip wear. Clinical Orthopaedics 333, 41–50.

Maxian, T.A., Brown, T.D., Pedersen, D.R., Callaghan, J.J., 1996c. A sliding-distance-coupled finite element formulation for polyethylene wear in total hip arthroplasty. Journal of Biomechanics 29, 687–692.

Maxian, T.A., Brown, T.D., Pedersen, D.R., McKellop, H.A., Lu, B., Callaghan, J.J., 1997. Finite element analysis of acetabular wear. Validation, and backing and fixation effects. Clinical Orthopaedics, 111–117.

Perez, R.E., Rodriguez, J.A., Deshmukh, R.G., Ranawat, C.S., 1998. Polyethylene wear and periprosthetic osteolysis in metal-backed acetabular components with cylindrical liners. Journal of Arthroplasty 13, 1–7.

Sauer, W.L., Anthony, M.E., 1998. Predicting the clinical wear performance of orthopaedic bearing surfaces. In: Jacobs J.J., Craig T.L., (Eds.,) Alternative Bearing Surfaces in Total Joint Replacement. ASTM STP 1346, American Society for Testing and Materials, West Conshohoken.

Schmalzried, T.P., Guttmann, D., Grecula, M., Amstutz, H.C., 1994. The relationship between the design, position, and articular wear of acetabular components inserted without cement and the development of pelvic osteolysis. Journal of Bone Joint Surgery American 76, 677–688.

Schmalzried, T.P., Kwong, L.M., Jasty, M., Sedlacek, R.C., Haire, T.C., O'Connor, D.O., Bragdon, C.R., Kabo, J.M., Malcolm, A.J., Harris, W.H., 1992. The mechanism of loosening of cemented acetabular components in total hip arthroplasty. Analysis of specimens retrieved at autopsy. Clinical Orthopaedics 274, 60–78.

Schmidt, P.N., Bartel, D.L., 1997. Effect of load angle on mechanical behavior of cemented acetabular cups. 1997 Bioengineering Conference (ASME) 35, 59–60.

Underwood, P., 1983. Dynamic relaxation. In: Hughes, T.J.R., Belytschko, T. (Eds.), Computational Methods for Transient Analysis. North-Holland, Amsterdam, pp. 245–267.

Wang, A., Stark, C., Dumbleton, J.H., 1995. Role of cyclic plastic deformation in the wear of UHMWPE acetabular cups. Journal of Biomechanical and Material Research 29, 619–626.

Wang, A., Sun, D.C., Yau, S.-S., Edwards, B., Sokol, M., Essner, A., Polineni, V.K., Stark, C., Dumbleton, J.H., 1997. Orientation softening in the deformation and wear of ultra-high molecular weight polyethylene. Wear 203–204, 230–241.

Williams, V.G.N., Whiteside, L.A., White, S.E., McCarthy, D.S., 1997. Fixation of ultrahigh-molecular-weight polyethylene liners to metal-backed acetabular cups. Journal of Arthroplasty 12, 25–31.

Xenos, J.S., Hopkinson, W.J., Callaghan, J.J., Heekin, R.D., Savory, C.G., 1995. Osteolysis around an uncemented cobalt chrome total hip arthroplasty. Clinical Orthopaedics 317, 29–36.